Some remarks on plasma spraying powder injection techniques

SOME REMARKS ON PLASMA SPRAYING POWDER INJECTION TECHNIQUES

By J. M. Houben (Senior Scientific Officer)
Eindhoven University of Technology, The Netherlands.

SUMMARY

In order to avoid or diminish the inhomogenity of a plasma sprayed deposit, two injection methods have been developed which allow a centerline injection of the powder, leading to rotational symmetry of plasma and spray jet. Starting from theoretical considerations concerning transport and injection of the powder, it appears to be logical to split up these two functions of the powder gas into two separately controllable functions. The new injection techniques are briefly outlined and some spray results, mainly concerning oxygen content, hardness, structure and appearance of the spray jet are given.

Applying these new techniques it is possible to reduce the oxygen content of sprayed molybdenum deposits at a spraying distance of 130 mm and 80 mm to respectively 1,6 and 1,0 weight %. These deposits have no more coarse oxide inclusions; the structure shows epitaxy and porosity is strongly reduced.

1. INTRODUCTION

The inhomogenity of a sprayed deposit depends largely upon the differences in the interaction of the separate spray particles with the plasma and the surrounding atmosphere. A different interaction leads to differences in heat- and gasabsorbtion, oxidation, acceleration and interaction of the particles with the substrate. The interaction is related to the trajectory of the particles.

The trajectories are mainly determined by three inputdata of the spraying process:

a. The spraying powder; shape, size, density.
b. The plasma; laminar, turbulent, chemical composition, enthalpy.
c. Injection technique; place of injection, velocity.

The aim of the work partly reported here, is to indicate how the injection technique especially influences the homogenity of a sprayed deposit. In order to isolate the effects of injection and particle size a molybdenum powderfraction of 44-53 micron size is chosen as a standard reference powder.

In conventional injection systems the powder is feeded nearly perpendicolar to the plasma jet. In order to control the dwell time of the particles, the powder port may also be tilted to a certain angle with the plasma jet.

The gas needed for the transport of the powder from powder feeder to torch is also used completely to inject the powder into the flame. These systems work reliably but they cause an asymmetric spray jet; the particles pass through the plasma and leave it at a certain angle, so that the spray jet and the plasma are not concentric. This problem is discussed by Scottland Cannell [1], Hantzsche[2,4] and Kranz [3]. In fact there are three overlapping streams of particles, see fig. 1 and 10a.

① Particles with such an injection impuls that they pass through the plasma jet.
② Particles which are centrally transported by the plasma.
③ Particles with to small an injection impuls. They are glanced off by the viscous plasma.

Only the particles of stream ② and some of stream ① give a fair to good quality of the sprayed deposit. Particle stream ① is first heated and then oxidized considerably during the flight in the surrounding atmosphere.

The particles of stream ③ are only partly molten. Nevertheless, they may stick to the substrate, causing porosity and weakness of the deposit.

Starting from those disadvantages of the conventional injection systems, it was the aim of the development of two new systems to obtain a rotational symmetric spray jet. The differences in interaction between particles, plasma and surrounding atmosphere should be reduced to an acceptable amount. Especially oxidation should be avoided as much as possible.

With respect to this last aim the oxygen concentration across a plasma jet has been measured at distances of 25, 50, 75 and 100 mm from the torch. As can be expected the O_2 concentration is less in the center of the gas stream, see fig. 2. As a consequence, it should be tried to inject the powder in such a way that the trajectories of the particles lie in the centerline area like indicated in fig.2.

System I. The powder is feeded perpendicular to or at a slight angle with the plasma as in conventional way. However, the injection velocity of the powder is controlled (in principle independent of the quantity of powdergas) in such a way thet the powder is no more shot through the plasma but reaches the centerline region of the plasma.

System II. The powder is feeded axially into the plasma through the cathode. The trajectories of the powder and the cathode spot emitting the electrons for the arc-discharge are separated. The adhering of molten powder particles to the injection bores is avoided.

2. POWDER TRANSPORTCONDITIONS

Previous to entering into the details of system I the flowconditions for the transport of the powder from feeder to torch should be known. The transport velocity of a powder particle is a boundary condition for attuning the proper injection impuls.

The quantity of powder gas that is needed to attain a stable powder transport is determined by the diameter of the transport hose, the density, size and shape of the powder, the density and velocity of the powder gas. It is possible to describe stable transport on the basis of fig. 3 and the two dimensionless Froude numbers

$$\overset{+}{Fro} = \frac{v_f}{\sqrt{gd_p}} \quad \text{and} \quad Fro = \frac{v_g}{\sqrt{gd_h}}$$

v_f = floating velocity of a particle in the transport gas. For a laminar gas stream, defined by the expression

$$v_f = \frac{gd_p^2\,(\rho_p-\rho_g)}{18\,\eta} \simeq \frac{gd_p^2\,\rho_p}{18\eta}$$

d_p = particle diameter
v_g = mean velocity of the powder gas
d_h = transport hose diameter
ρ_p = powder dencity
ρ_g = density of the powder gas
η = dynamic viscosity of the powder gas

$\overset{+}{Fro}$ takes into account the material properties of the spray material and the powder gas. Fro refers to the flowconditions such as gas velocity and hose diameter. From fig.3 it is evident that the additional resistance of a gasstream when carrying powdered material (indicated by the resistance coëfficient λ_z) decreases with increasing Fro number. From a certain Fro number, λ_z even remains nearly constant.

Some numerical values based on Molybdenum as a spray material and argon as a powder gas are summarized in table 1.

Table 1: Floating velocities and Froude numbers related to the transport of Mo in argon gas[a]

Particle diameter µm	10	30	50	90
v_f ms^{-1}	0,026	0,234	0,666	2,158
$\overset{+}{Fro}$	2,6	13,6	30,0	72,6[b]
Fro ≥	35	35	45	75

a ρ_{Mo} = 10200 kg m^{-3} ;
ρ_A = 1,78 kgm^{-3}
η_A = 2,096.10^{-5} NSm^{-2}

b extrapolated in fig. 3.

Based on these figures the minimum average gas-velocities and the minimum gasquantities needed for a stable transport are calculated for powder hoses with diameters 1,5; 2; and 4 mm; see fig. 4.
The choice of a powder hose will also be based upon the maximum transport capacity for a certain amount of gas. The transport capacity according to Eck[5] is given by

$$\mu = \frac{\phi_{mp}}{\phi_{mg}} = C.\ Fro^4$$

μ = ratio of the powder massflow ϕ_{mp} to the mass of the gasflow ϕ_{mg}
C = constant ≈ 3.10^{-5}
For hoses with diameter 1,5; 2 and 3 mm. ϕ_{mp} can be calculated on the basis of the Fro numbers of table 1, viz based on the necessary minimum gasquantities; see table 2.

Table 2: Powder mass flow ϕ_{mp} $gmin^{-1}$ based on minimum transport gas quantities.

d_h mm \ d_p µm	10	30	50	90
1,5	36	36	126	1623
2	74	74	259	3343
3	203	203	715	9203

From this table it is obvious that a hose with a diameter of 2mm has got sufficient transport capacity for commercial plasma spraying. The device which is mentioned in this paper has been equipped with a hose of 3 mm.
Summarizing: the transport conditions for molybdenum and argon as a powdergas are given in the figures 3 and 4 and the tables 1 and 2.

3. INJECTION CONDITIONS, TRAJECTORIES AND VELOCITIES OF SPRAY PARTICLES

In order to calculate the trajectory of a powder particle that is shot into a plasma stream, the conditions of state of the plasma such as temperature (T_{pl}), density (ρ_{pl}), viscosity (η_{pl}) and the velocity (C) should be known as a function of x, y, z coördinates.The particle

should have, at least, a well defined mass however by ablation and oxidation the mass of a particle will not be a constant. Besides the shape of a particle will change during the flight through the plasma and there is some uncertainty about the drag coefficient of a particle in a plasma stream, the more so as a plasma flame for spraying operation may consist of laminar and turbulent zones. So the determination of the required injection velocity on theoretical basis must be seen as an attempt to find out the relations between the relevant parameters which are of importance for the injection velocity. Suppose that 1 the plasma has got a diameter D and length L (see fig.1) 2 the temperature, plasma velocity, density and viscosity are uniform within the plasma volume and 3 the earth's gravity can be neglected. Further, suppose that the powder particle may be considered like a sphere. At least the spherical shape will be reached in the plasma by ablation and melting.
The Reijnolds number for a particle in a plasma stream is defined by

$$Re = \frac{\rho_{pl} \cdot C \cdot d_p}{\eta_{pl}}$$

An arbitrary but characteristic argon plasma has the following properties[6,7]:

$T_{pl} = 10806$ K; $\rho_{pl} = 0{,}0417\ \frac{kg}{m^3}$; $C = 500\ \frac{m}{s}$;

$\eta_{pl} = 33.10^{-5}\ \frac{NS}{m^2}$

So, the Re-numbers can be calculated from $Re = 0{,}63.10^5\ d_p$.
For 10 μm < d_p < 90 μm holds: 0,63 < Re < 5,67. Based upon these Re numbers, Stokes'law for the drag coëfficient of a particle is supposed to be valid.
For this plasma, the velocity and the trajectory of a particle can be described bij the following equation:

$$V_{py} = v_{ip} \exp\left[\frac{-3\pi\eta_{pl}\, d_p}{m_p} . t\right] \qquad (1)$$

$$y_p = \frac{m_p v_{ip}}{3\pi\eta_{pl} d_p}\left[1 - \exp \frac{-3\pi\eta_{pl}\, d_p}{m_p} . t\right] \qquad (2)$$

$$v_{px} = C\left[1 - \exp \frac{-3\pi\eta_{pl}\, d_p}{m_p} . t\right] \qquad (3)$$

$$x_p = Ct - \frac{Cm_p}{3\pi\eta_{pl} d_p}\left[1 - \exp \frac{-3\pi\eta_{pl} d_p}{m_p} . t\right] \qquad (4)$$

Notation: If the expression for the floating velocity

$v_f = \frac{g\, d_p^2 \rho_p}{18\ \eta_{pl}}$ is used, then $\frac{m_p}{3\pi\eta_{pl} d_p} = \frac{v_f}{g}$

To facilitate the performance of numerical calculations the following definitions turn out to be usefull:

$A_p = \frac{3\pi\eta_{pl} d_p}{m_p}$, so $A_p = \frac{g}{v_f}$

Numerical values for A_p based on molydenum are given in table 3.

Table 3 : numerical values of A_p, T_{max} and v_{ip} for molybdenum and argon plasma.

d_p	μm	10	30	50	90
A_p	s^{-1}	5839	649	233	72,1
t_{max}	S	$2{,}13.10^{-4}$	$5{,}62.10^{-4}$	$9{,}12.10^{-4}$	$17{,}58.10^{-4}$
v_{ip}	ms^{-1}	28,6	7,4	4,2	2,1

Using the definition of A_p, the equations (1-4) can be written as follows:

$$v_{py} = v_{ip} \exp -A_p . t \qquad (1a)$$

$$y_p = \frac{v_{ip}}{A_p}\left[1 - \exp - A_p t\right] \qquad (2a)$$

$$v_{px} = C\left[1 - \exp -A_p t\right] \qquad (3a)$$

$$x_p = Ct - \frac{C}{A_p}\left[1 - \exp -A_p t\right] \qquad (4a)$$

A characteristic time for the trajectory of a particle is the dwell time in the plasma: t_{max} .
If $t = t_{max}$ it holds: $x_p = L$ and for centerline injection the y coördinate must satisfy:

$y_p = \frac{D}{2}$

The equations (4a) and (2a) become:

$$L = Ct_{max} - \frac{C}{A_p} (1 - \exp - A_p t_{max}) \qquad (5)$$

$$\frac{D}{2} = \frac{V_{ip}}{A_p} (1 - \exp -A_p t_{max}) \qquad (6)$$

The time t_{max} can be calculated from (5). Substitution of t_{max} into equation (6) yields the value of v_{ip} . This v_{ip} satisfies the requirement of centerline injection.
The results of the calculations for t_{max} and v_{ip} are summarized in table 3 and fig.4.

The trajectory of a particle in x-y coordinates can be yielded from (2) and (4) if time is eliminated

$$\frac{x_p A_p}{C} = \ln \left[\frac{v_{ip}}{v_{ip} - A_p y_p} \right] - \frac{A_p y_p}{v_{ip}} \qquad (7)$$

With centerline injection there are two fixed points of the trajectory: $(x_p, y_p) = (0,0)$ and $(x_p, y_p) = (L, \frac{D}{2})$.

Furthermore x_p as a function of particle diameter is calculated for $y_p = 0{,}1D$; $0{,}2D$; $0{,}3D$ and $0{,}4D$ respectively. See fig. 5.

In these calculations v_{ip} is chosen according to fig.4.

The angle ϕ between trajectory and the centerline of the plasma is determined by the velocities v_{px} and v_{py}. For centerline injection VIZ. $x_p = L$ and $y_p = \frac{D}{2}$, holds:

$$\tan \phi = \left[\frac{v_{py}}{v_{px}} \right]_{t_{max}} \qquad (8)$$

$$\left[\frac{v_{py}}{v_{px}} \right]_{t_{max}} = \frac{v_{ip}}{C} \cdot \frac{\exp -A_p t_{max}}{1 - \exp -A_p t_{max}} \qquad (9)$$

Results are given in fig. 6.

The velocity v_{px} of a particle leaving the plasma is calculated with equation (3a). The results are also given in fig. 6.

The following concluding remarks can be made now:

Fig. 4 : For centerline injection the injection velocity is strongly related to the particle size. This holds especially for particles smaller than 50 µm.

5 : If proper injection velocity according to fig. 4 is applied, the trajectories do not depent strongly on the particle size. In the beginning small particles show a slightly greater (∿ 0,08 D)penetration depth than large particles.

6a : When applying centerline injection the angle between the trajectory and the centerline of the plasma is small. For the particle size range from 20 to 90 µm holds: $1{,}78^o < \phi < 2{,}02^o$.

6b : The velocity v_{px} is strongly dependent of particle size.

Equation (2):
The penetration depth y_p is proportional to the injection impuls, $m_p v_{ip}$ of the particle. For a fixed particle size, the dependance can be reduced to the influence of the injection velocity. In practice the particles will have a relative broad size range for commercial reasons. For such a powder the injection impuls of the particular particles is significant for the trajectories.

Summarizing: An injection system ought to be supplied with an injection impuls control which, in principle must be independent of the powder gas flow.

In the following section two systens which can meet this requirement are briefly outlined.

4. INJECTION SYSTEMS

After calculating the theoretically required injection velocities it is of interest how the real injection velocities are related to the minimum powder gas flow as given in fig. 4.
Beside the powder gas flow, the injection velocity of the powder will depend on size and shape of the injection mouthpiece.
The injection velocities have been measured in the following way. The mouthpiece to be tested is placed vertically thus allowing the powder gas with powder to flow out freely.
The velocity and the vertically covered distance of the powder are given by the equations:

$$v_p = \frac{-g}{A_{pa}} + (v_{ip} + \frac{g}{A}) \exp -A_{pa} t \qquad (10)$$

$$y_p = -\frac{g}{A_{pa}} t + \frac{1}{A_{pa}} \cdot \left[v_{ip} + \frac{g}{A_{pa}} \right] \cdot \left[1 - \exp -A_{pa} t \right] \qquad (11)$$

At the moment that y_p reaches the maximum height, $v_p = 0$. So, for maximun y_p Holds:

$$\frac{\exp \frac{A_{pa}}{g} v_{ip}}{\frac{A_{pa}}{g} v_{ip} + 1} = \exp \frac{A_{pa}^2}{g} y_{pmax} \qquad (12)$$

From equation (12) the maximum value for v_{ip} can be calculated when y_{pmax} has been measured. A_{pa} is defined by the expression

$$A_{pa} = \frac{3\pi\eta_{air} d_p}{m_p}$$; numerical values for A_{pa} based on Molybdenum and air have been listed in table 4.

Table 4.: Numerical values of A_{pa}.

d_p µm	90	75	63	53	45
A_{pa} s^{-1}	4,04	5,82	8,25	11,65	16,16

The variation in size and shape of the injection mouthpiece has been achieved by supplying it with internal diameters of 2 and 3 mm and a straight or (over 360°) curved shape.

The total length of the mouthpiece is constant: 120 mm.
Applying these 4 mouthpieces, y_{pmax} and v_{ip} have been determined for the powder gas flow 5,4; 4,3; 3,8 and 3,0 Nl/min. These quantities represent the minimum gas flows according to fig. 4 which are necessary for stable transport of Molybdenum particles with diameters up to 90; 75; 63; 53 and 45 µm respectively. The powder gas flow of 5,4 l/min is applied moreover for transport of all the above mentioned size ranges.
To elucidate matters the measuring scheme for the straight injection mouthpiece with 3 mm diameter is given in table 5.

Table 5 : Measuring scheme for the determination of y_{pmax} (mm); straight injection mouthpiece; 3 mm diameter.

ϕ_v Nl min^{-1} \ d_p µm	90	75	63	53	45
5,45	710	710	710	700	750
4,35		630			
3,80			510		
3,40				460	
3,0					510

Fig. 7 shows the calculation results for v_{ip} based on the above described y_{pmax} measurements. From this figure it appears that the measured values of v_{ip} surpass considerably the theoretically required values based on centerline injection. Increasing the flow resistances of the mouthpiece, by introducing the 360^o winded one and lowering the powder gas flow, are effective to diminish the discrepancies, especially so for small particles. However reducing the powder gas flow, implies also that coarse grains cannot be transported as appears from fig. 4.
The proper quantity of powder gas, although restricted to the minimum, still surpasses the powder gas flow which is needed for centerline injection. So, it is obvious to split up the transport- and injection function of the powder gas into two separately controllable functions as has been introduced in the new injection system I^+, schematically given in fig. 8. This system comes to this, that the quantity of powder gas, ϕ_{V1}, is reduced with an amount ϕ_{V2}, after the powder gas has fullfilled the transport function and at the beginning of the injection function. The gas flow ϕ_{V2} is adjustable, so that any gas flow ϕ_{V3} needed for the injection can be obtained. With this injection system a rotational symmetric spray jet has been achieved.

\+ patents pending.

Another injection system II^+ which also produces a rotational symmetric spray jet is sketched in fig. 9. In this system the powder is feeded axially into the plasma via 4 or 6 bores annularly situated around the cathode spot. Besides, the ring of bores has been placed a few milimeters backwards of the cathode spot.

\+ patents pending.

The heart of this construction is represented by the fact that powder trajectory and cathode spot do not coincide. For that reason the powder will not stick to the hot cathode as is the case when a quite simple construction such as acentral bore through the cathode is applied. To overcome the counter pressure of the plasma a slightly increased powder gas flow is necessary for injection. So, problems with respect to transport and injection gas flow as described in the previous method do not exist. However the system is not as versatile as method I. Low melting point materials such as Sn, cannot be handled with it and the anode bore must be restricted to values from approximately 8 mm at the least.

5 SPRAY RESULTS, DISCUSSION.

Some spray results are listed in table 6.

Table 6: Some spray results.

System	I		II		spray material
Spray distance mm	80	130	80	130	Mo
O_2 % weight	1,01 1.03 0,96	1,61 1.59 1,59	0,82 0,84 0,98 1,0	1,59 1,56 1,62 1,60	0,149 0,142 0,147
Vickers microhardness H_{V25} at distance x from substrate kgf mm^{-2}.					
x µm					
20	424	488	413	642	275
50	424	627	424	519	
80	386	673	370	560	
110	363	657	473	612	
140	383	627	429	606	
170	417	503	354		
200	363	525	424		
230	397	548	351		
260	386	572	311		
290	424	627	376		
320	333	599	336		
350	405	612	383		
380	357		437		
410	413				
Average	391	588	390	587	
Heat content kJ kg^{-1}	-	1200	-	1050	

Photographs of the spray jet, fig.10, show that in these new systems the plasma and the particle jet coïncide symmetrically.
Both injection systems lead to relatively low oxygen contents of the deposits. There is an increasing hardness with increasing spraying distance, directly related to the oxygen content. This can be concluded from the microhardness figures.
The deposits do not show coarse oxide inclusions. So, in the absence of these material and thermal barriers, adhesion to the substrate and cohesion of the lamellae might be increased. At this moment exact figures about the mechanical properties are not yet available.
From microanalysis, fig. 11, it is clear that the molybdenum is bounded to the substrate via an intermetallic phase accompanied by diffusion zones in both the Mo deposit and the Fe substrate. The micro photographs, fig. 12, show the structure of the deposit in both unetched and etched condition. Especially from the unetched structure, shown with a small magnification, an impression can be gathered about the slight porosity of the deposits.
The etched structure shows good adhesion between the separte lamellae.
As research is still in progress, full details about the thermal analysis of the spray particles do not yet exist. Nevertheless a tentative conclusion can be drawn for a powerlevel of approximately 12 kw over the electrodes and a spray distance of 130 mm.
Conversing the heat contents of table 6 into temperatures of the spray particles it appears that, using system I, all particles can be completely molten and even superheated slightly.
When using system II, some particles will remain just partly molten and superheating will probably not occur at this powerlevel.
Among other things, the reasons for the discrepancy in heat absorption of the particles will be cleared up in progress of this research.

6 CONCLUSION

Two powder injection systems for plasma spraying have been worked out, which produce a rotational symmetric confined jet of particles.
Applying these systems to the spraying of molybdenum, it appears that the oxygen content and the porosity of the deposit can be restricted and the homogenity can be improved considerably without using high power levels.

7 ACKNOWLEDGEMENT

The author is gratefull to mr. G.G. van Liempd and P.L.H.de Waal for their assistance in thinking about the theoretical aspects and the performance of practical work involved in this investigation.

8 REFERENCES

1. Scott. B.F. and Cannell J.K. Arcplasma Spraying- an analysis. Int. J. Mach.Tool Des.Res. Vol. 7, 1967, pp. 243-256.
2. Hantzsche.H.Untersuchungen über optimale Transportbedingungen beim Plasmaspritzen von Wolframkarbidpulver. Wissenschaftliche Zeitschrift Th. Ilmenau 15 (1969).Heft 3,pp. 99-106
3. Kranz.E. Untersuchungen über das Einbringen von Zusatzsubstanzen in lichtbogenplasmen. Wissenschaftliche Zeitschrift Th.Ilmenau 16 (1970).Heft 23 pp. 181-188.
4. Hantzsche. H. Bedeutung der Pulverförder-geschwindigkeit beim Plasmaspritzen.Schweisstechnik 21 (1971). Heft 9. pp 399-403.
5. Eck. B. Technische Strömungslehre. Springer Verlag Berlin. 1966.
6. Houben J.M. and Zaat J.H. Analysis of a plasma torch. Paper 28. Proc. 7th Metal Spraying Conference, London 1973.
7. Amdur .I. and Mason. E.A. Properties of gases at very high temperatures. The physics of fluids. Vol. 1, Nr. 5, 1958, pp. 370-383.

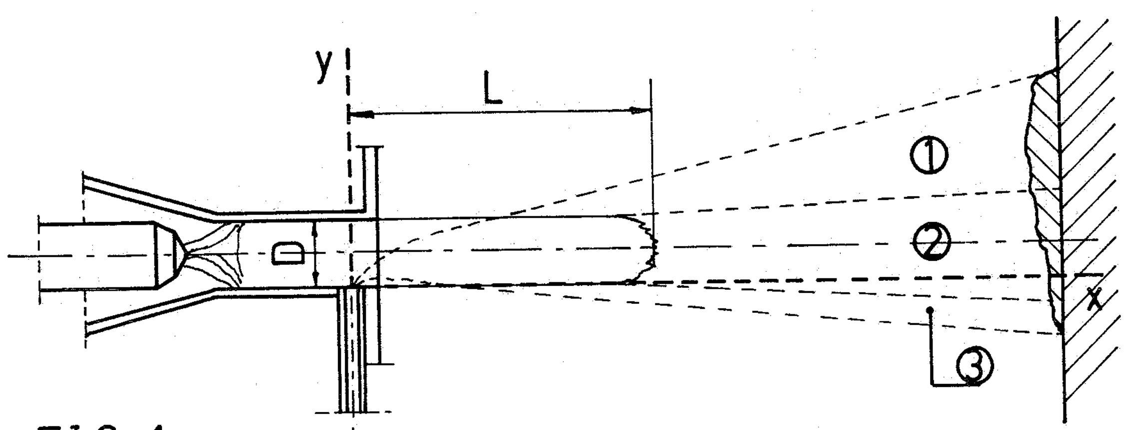

FIG. 1
basic concept of plasma spraying

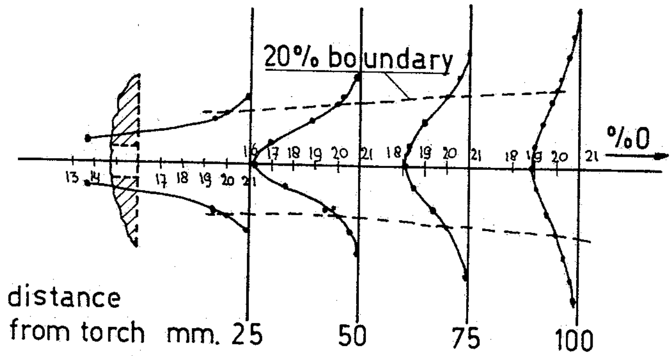

FIG. 2
oxygen content of spray gas

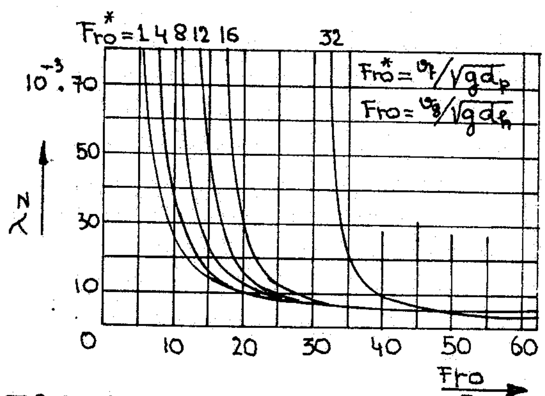

FIG. 3 according to Eck[5]
Froude numbers for vert. transport of powdered material;
flow resistance coëff λ_z

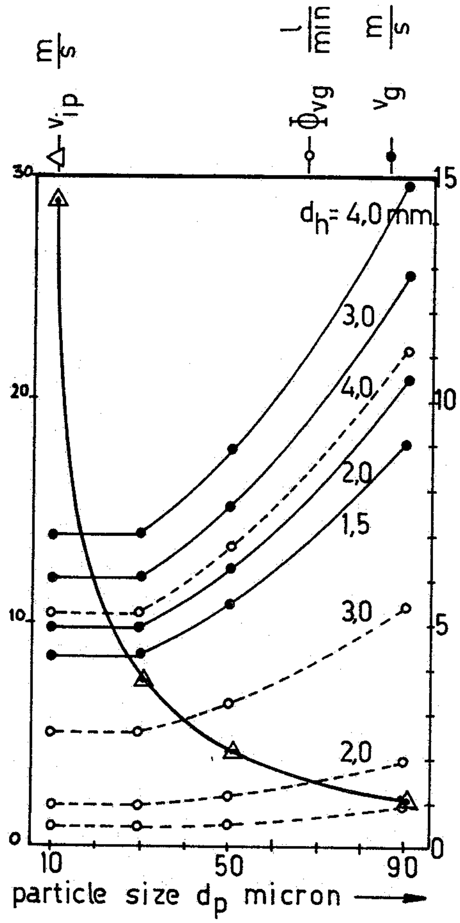

FIG. 4
minimum powdergas-flow and velocities for vert. transport of molybdenum.
minimum injection-velocity for m_0 in argon plasma

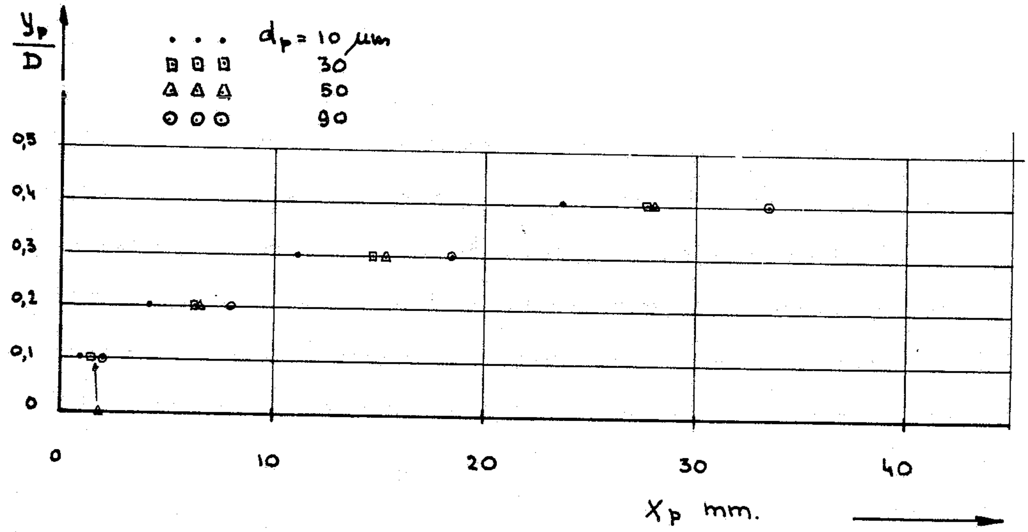

FIG. 5 Trajectories of molybdenum particles in argon plasma applying centerline injection.

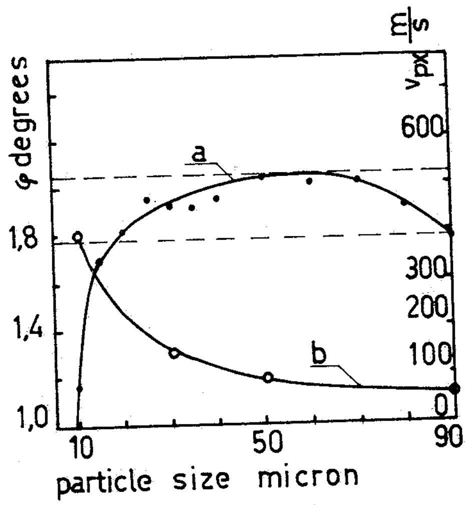

FIG. 6a : angle φ between trajectory and plasma center-line; $\varphi = \arctan(v_{py}/v_{px})_{x=L}$
6b : particle velocity v_{px}

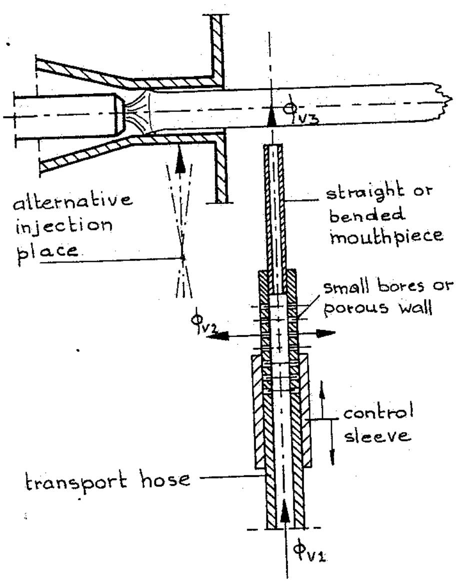

FIG. 8 : injection system I provided with injection impuls-control

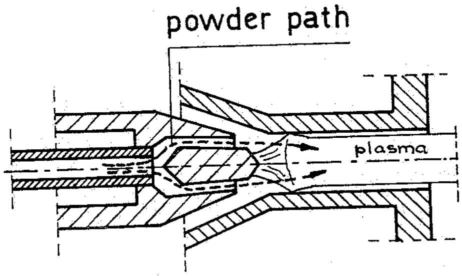

FIG. 9 : injection system II

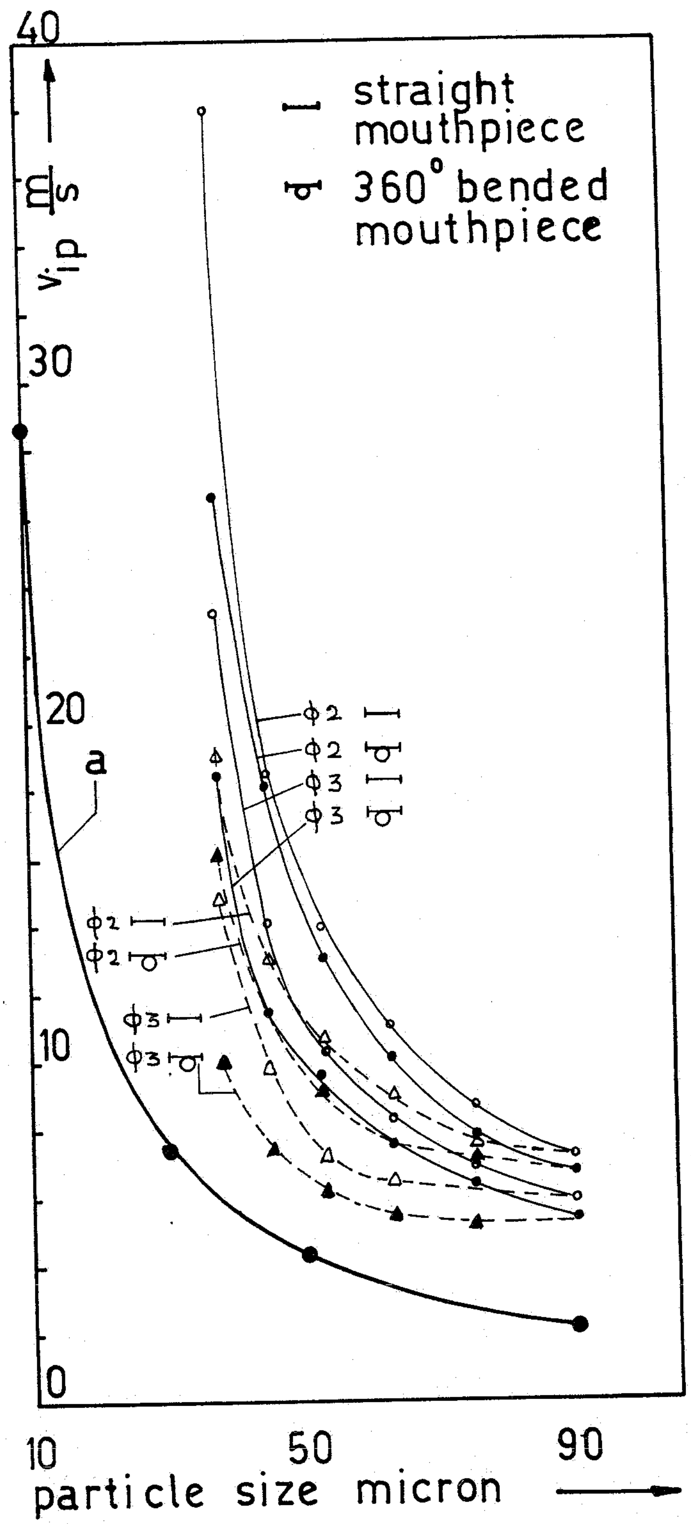

FIG. 7: measured injection velocities

- Full lines:powder gas-flow based on stable transport requirements for Mo particles up to 90 micron.
- Dashed lines: reduced powder gas-flow (acc. to table 5).
- Curve a : Theoretically required centerline injection velocity.

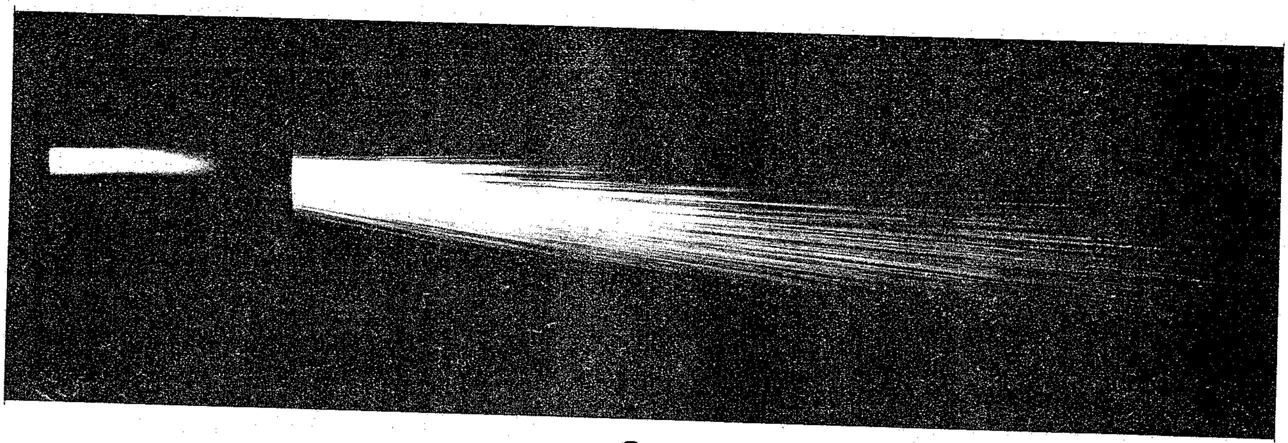

a

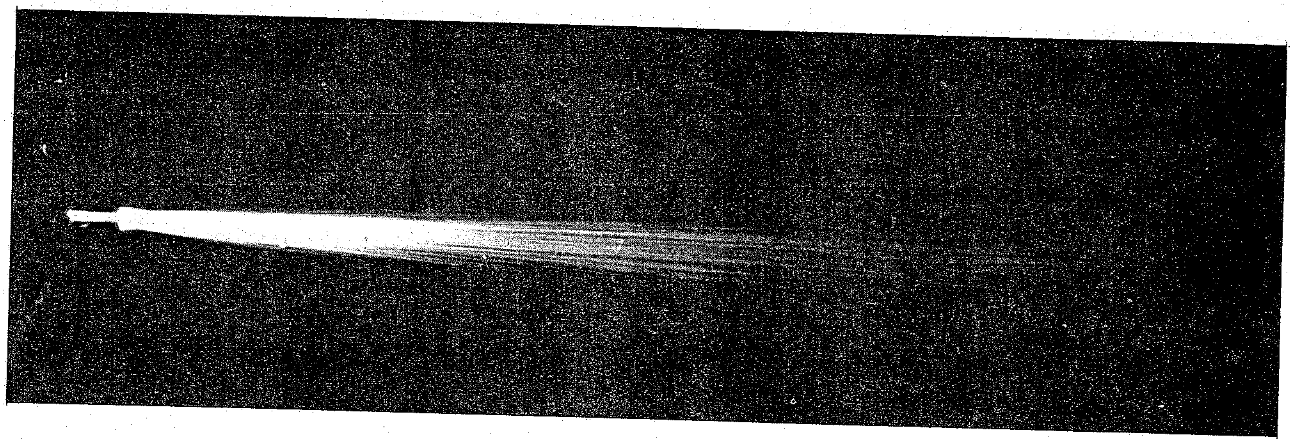

b

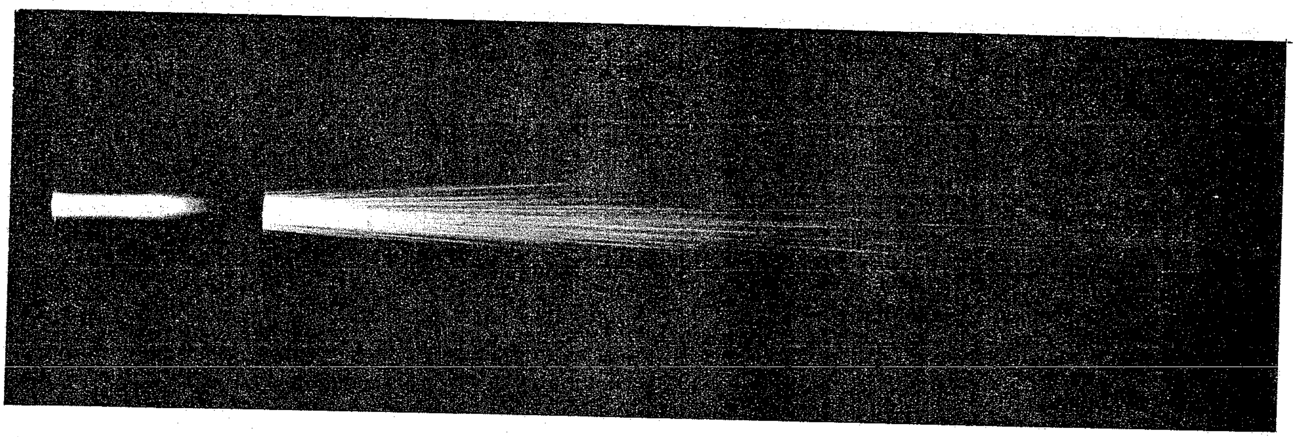

c

FIG.10

a. Spray jet using conventional injection method
b. Spray jet using injection method with injection impuls control, system I.
c. Spray jet using axial powderfeed system II

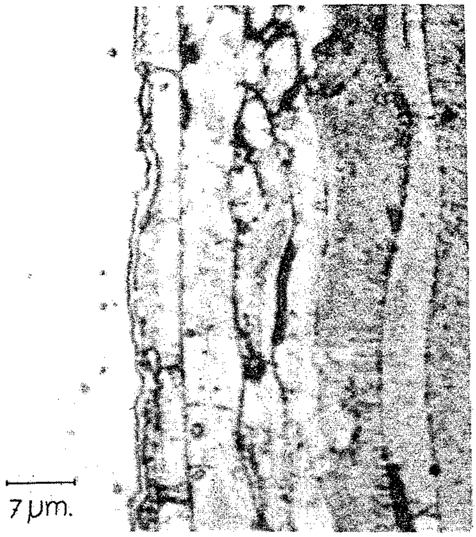

a. Microphotograph showing an intermetallic layer in the adhesion zone, using injection system I

FIG. 11

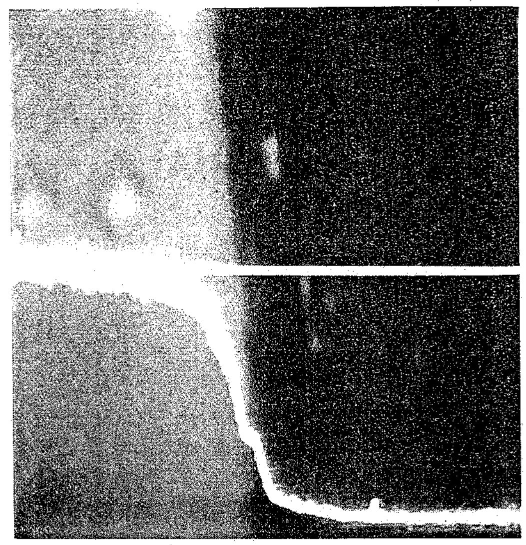

b. K_α-Fe line scan showing Fe concentration across the adhesion zone.

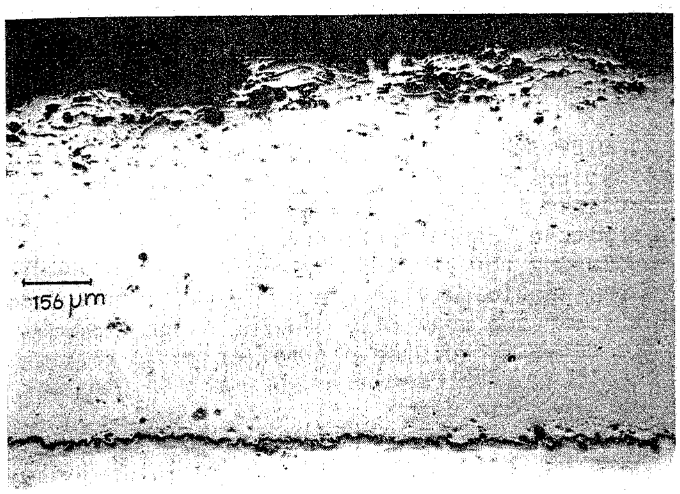

a. Using system I, unetched, spraying distance 80 mm,oxygen content 0,9-1,1%.

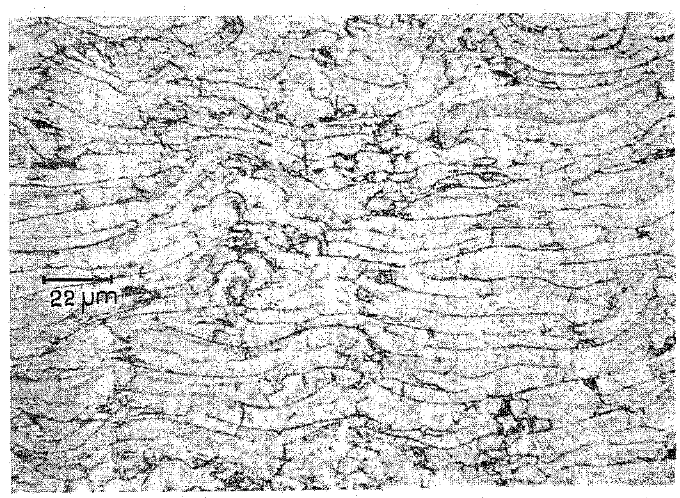

b. Using system I, detail of 12a etched with Murakami's reagent.

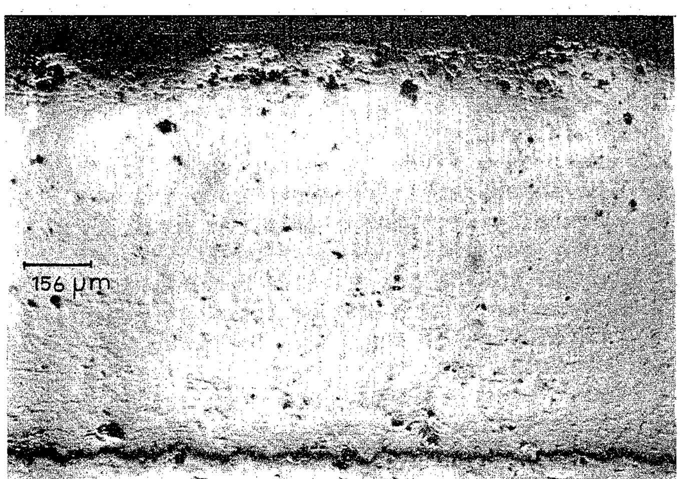

c. Using system II, unetched, spraying distance 80 mm, oxygen content 0,9-1,1%

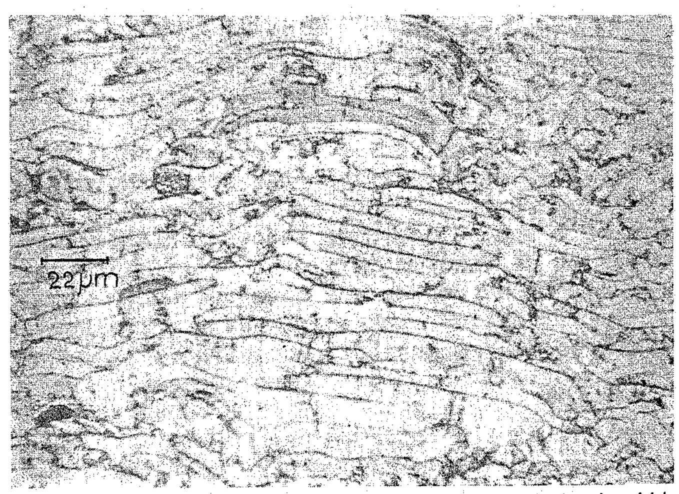

d. Using system II, detail of 12 c etched with Murakami's reagent.

FIG.12 Photomicrographs of the structure of Mo deposit